Chapter 3.

THE PERFORMANCE OF THE ANALYSER: FIELD ADSORPTION.

3.1.1 Alignment.

The full resolution of the energy analyser is only attained when the focal plane of the ion beam coincides with the input side of the channel-plate detector. Once an unfocussed beam of image-gas ions had been obtained on the detector the analyser could be focussed accurately by an iterative adjustment of the mechanical positions of the tip, the screen, and the detector. The beam was generally focussed using the helium field-ion signal from a bright part of the specimen, at best image voltage. The energy spread of the helium ions at BIV is known from the work of previous investigators, outlined above, to be of the order of 1 volt or less. A comparison of the relatively well focussed and grossly unfocussed conditions is shown in fig (3.1). It should be noted that in the photographs of the detector output shown here and elsewhere, the energy scale is vertical, with the lowest energy ions producing scintillations at the top of the detector. The analyser focusses the ion beam in one dimension only, so a (diverging) monoenergetic beam of ions arrives along a line on the detector. The curvature of this line, as explained above, is partly due to fringing fields at the entrance and exit slits of the condenser.

Care was necessary when aligning the spectrometer to ensure that a false focus was not obtained. Such foci may be reached when:-

a) the beam-angle is reduced by intersection with the edge of one of the apertures in the system

Fig. 3.2

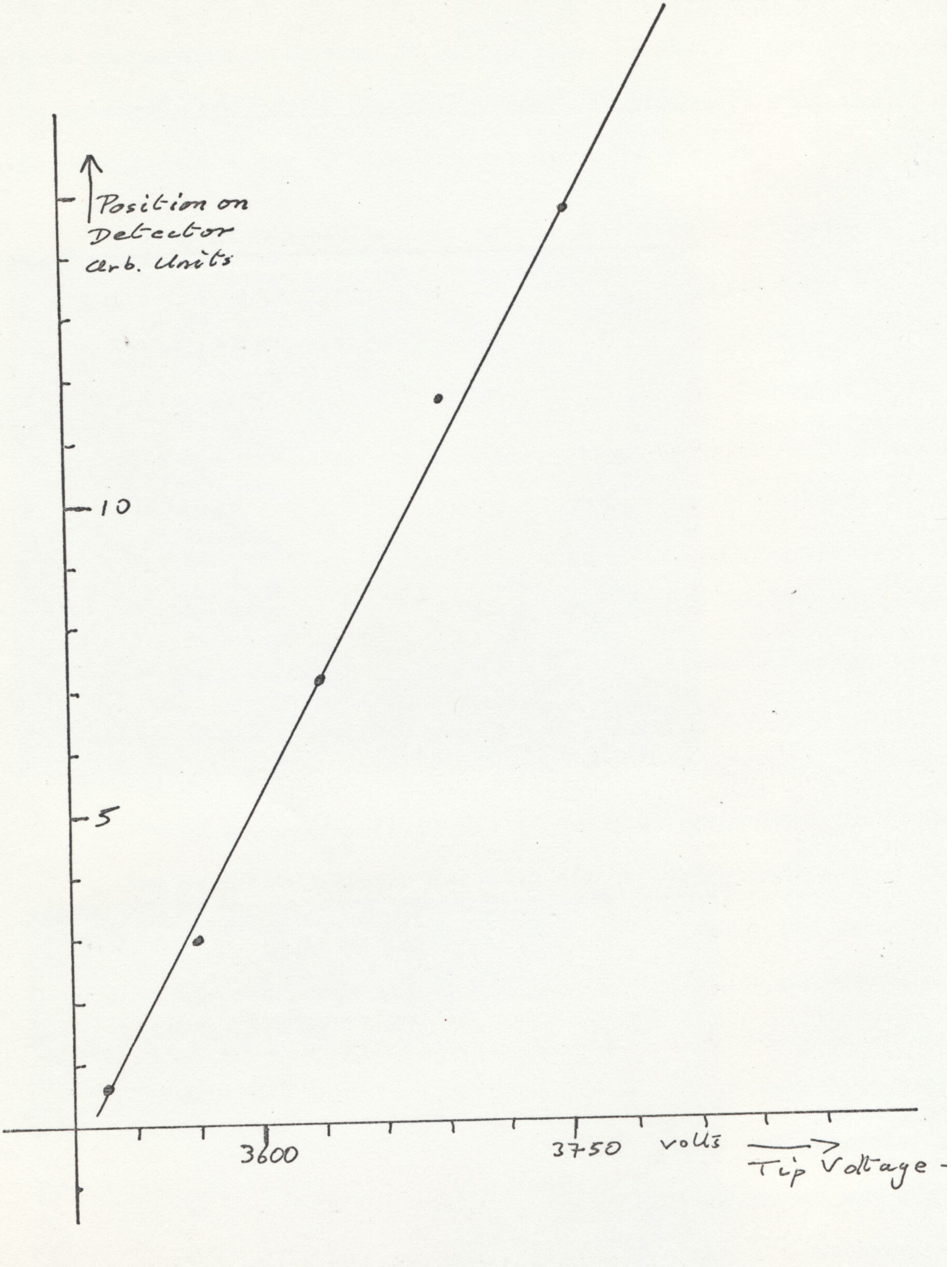

Position on Detector arb. units
10
5
3600
3750
volts
Tip Voltage

b) the focal plane of the beam intersects the detector at an angle, so that a sharp focus is only obtained at one point of the detector

c) the probe-hole aperture is only partially illuminated by one small, brightly emitting, area of the specimen. This has the effect of artificially reducing the divergence of the beam, so the resolution of the analyser ($1.6\Delta\theta^3$) is apparently improved. As soon as the probehole is moved to a uniformly emitting area the analyser is seen to be out of focus. Equally, if two separate emitting areas of the specimen lie under the probehole of the out-of-focus analyser, an artificial splitting of the energy spectrum into two peaks may be obtained.

3.1.2 Linearity and Dispersion.

The linearity of the analyser was checked by measuring the position on the detector of the spectral line as a function of specimen voltage, at a fixed analyser voltage. The results are plotted in fig (3.2). As may be seen, the plot is linear, within the accuracy of the measurements. The dispersion measured from this graph corresponds well with the theoretical value (0,175 mm./volt).

3.1.3 Stray Magnetic Fields.

In any ion-optical system there may be unacceptable deflections of the ion beam by stray magnetic fields. An ion of charge ne which has been accelerated by a potential E will be deflected into a path with a radius

$$r = \frac{m\,v}{neB} = \frac{1}{B}\sqrt{\frac{2\,m\,E}{n\,e}}$$

where B is the magnetic field.

For small deflections the beam will be deflected sideways by a distance $L^2/2r$ after a flight of distance L. In the case of the energy analyser the beam is striking the detector at a glancing angle of incidence, and the observed deflection will be approximately

$$D = \frac{L^2}{2r} \cdot \frac{1}{\sin(30^\circ - 11^\circ)} \quad .$$

The magnetic field in the vicinity of the prototype analyser was investigated using a Hall-effect gaussmeter. The relevant component of the magnetic field was found to be around 10^{-5} T and was reduced to $6 \cdot 10^{-6}$ T by reorienting the analyser. The direction of this field was in a direction such as to deflect the positive ions towards the low-energy end of the spectrum. The calculated deflections for various ions are tabulated below, for E = 10 KV.

	m/n	D,mm	ΔE,volts
H^+	1	0,24	4,27
He^+	4	0,12	2,14
Ne^+	20	0,038	0,68
W^{3+}	61,3	0,031	0,55
Mo^{2+}	48	0,035	0,62
Mo^{3+}	32	0,031	0,55

3.1.4 Resolution.

The energy resolution of the analyser may be tested by energy-analysing the field-ion current produced by a mixture of helium and neon, at a suitable field. The two gases will produce ions from their respective critical distances with energy deficits

Fig. 3.3

Illustrating the resolution of the helium and neon field-ion energy-spectra. Each ion produces one of the scintillations recorded in the photograph of the detector output.

a) Neon alone

b) Neon and helium together

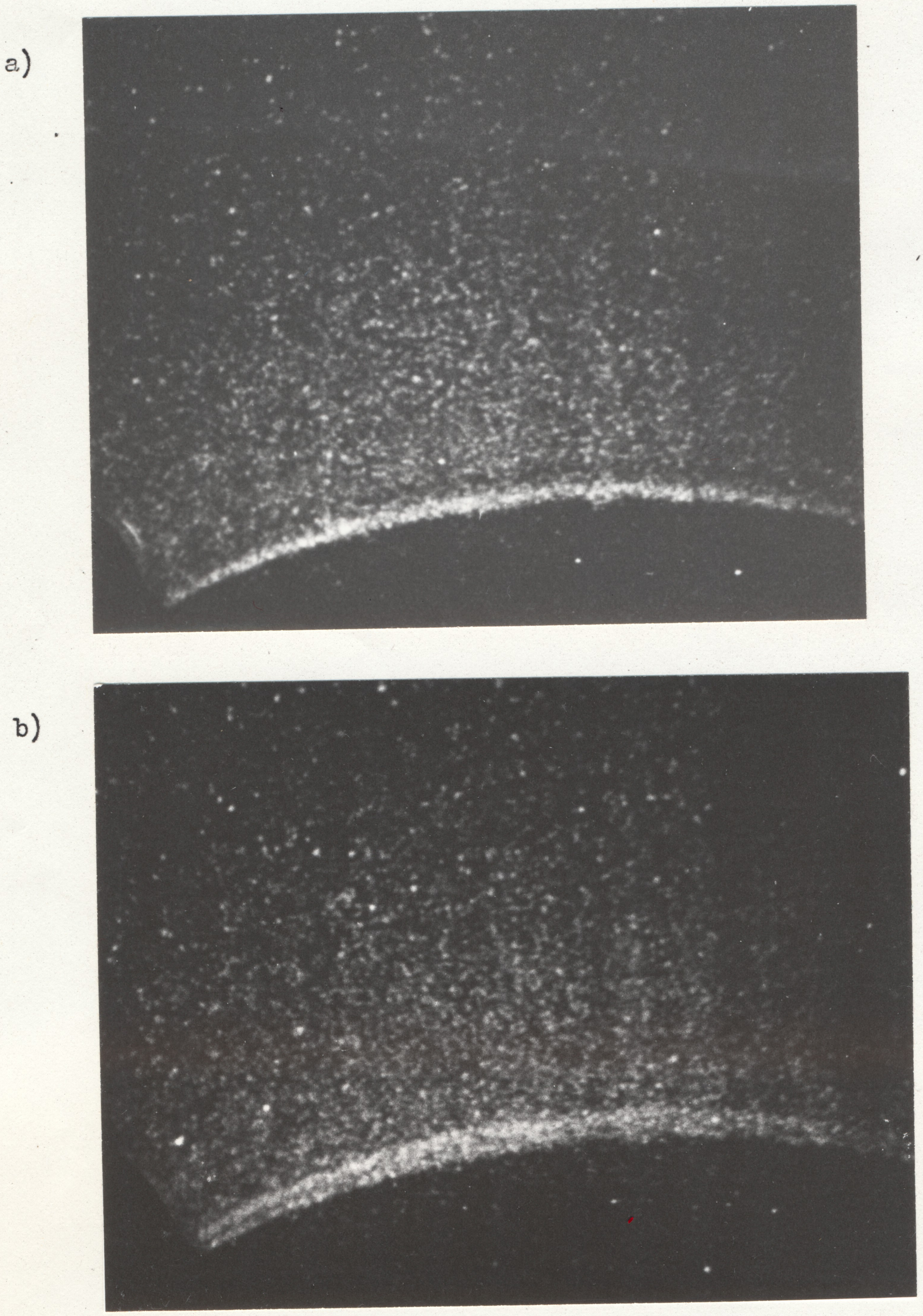

of approximately (I − Ø) where Ø is the metal work function and I is the gas ionization potential. The highest energy ions of the helium and neon will there fore be separated by a gap of ~

$I_{He} - I_{Ne} = 24{,}46 - 21{,}47 \simeq 3$ eV.

Fig (3.3a) shows a field-ion energy spectrum from neon alone. There is seen to be a narrow high-intensity high-energy line corresponding to ionization at the critical distance. As expected, there is also a long tail to the low-energy side of the main peak, corresponding to ionization further from the surface, since the field used for this experiment was relatively high(well above neon BIV). When helium is added to the system a second bright line appears in the spectrum (fig(3.3b)). This line corresponds to the ionization of helium at its critical distance, and remains undisturbed when the neon is pumped from the system. The resolution of the 3volt separation of the neon and helium lines at a specimen voltage of ~6KV implies an energy resolution of $\Delta E/E \simeq 5\,10^{-4}$ after making some allowance for the effect of magnetic fields. This compares quite favourably with the theoretical resolution for a perfectly aligned spectrometer of $\sim 10^{-4}$.

3.1.5 Recording Time and Detector Noise.

Useful records of field-ion spectra could be obtained with film exposure times of between a fraction of a second and some tens of seconds, depending on the intensity of the feature under study. The channel-plate gain could be reduced to obtain a spectrum from a very large number of ions without saturation of the film, at the expense of losing any very faint peaks in the spectrum. This also reduced the background noise from the channel-plate, which limited exposure times for field-ion signals to 30 seconds or so, when operated at high gain. A more serious noise problem with the field-ion signal was caused by 'signal induced noise'. This was the occurrence of a random faint background signal which only appeared in the presence of a bright field-ion signal. This was probably due to secondary electrons liberated from surfaces touched by the beam, or to ions scattered from such surfaces. This background noise was independent of pressure at a sufficiently low pressure, and was therefore not due to gas-phase collisions. The background detector noise could in principle be removed by using a low-light-level TV camera interfaced to a multichannel-analyser to store the spectrum digitally, so that a very large number of ions could be detected and stored, and so that the background noise level could be subtracted from the total. Signal-induced noise can only be removed by removing the source of the noise (eg by using a weak electric field to repel secondary electrons away from the detector).

In the case of experiments involving the detection of a few field-evaporated ions at widely-scattered energies, any background noise was felt to be unacceptable. The pulser used to evaporate the ions was therefore triggered by the electronic-flash shutter contacts on the camera, using a 1/60 second exposure. This reduced the background noise level, measured from blank experiments, to around 5 or less random signals over the whole channel-plate area.

3.2 Suitable Experiments for the Prototype Analyser.

It was shown in Chapter 2 that experiments on field ionization can be very sensitive to the presence of contaminants in the vacuum system. For this reason, the (relatively) poor vacuum of the prototype analyser limited the use of the analyser to experiments insensitive to small traces of contaminants; that is, to experiments at high fields using refractory metal specimens, so that the field itself would provide a barrier to the contaminants, and at high pressures of the gases involved in the experiment, so that contaminant effects would be swamped.

A further limitation, which was accepted when the analyser was designed, was in the resolution of the analyser; this was intended to be suitable for the measurement of the energies of field-evaporated ions, under pulsed conditions. As has been demonstrated by Utsumi (1973) there are interesting experiments to be performed on, for example, the detailed shape of the spectral line obtained at best image field. However, these experiments require an analyser with a resolution of 0.1 eV or better: although the parallel-plate analyser could be made to operate with a resolution approaching this, by restricting the angular divergence of the beam accepted by the analyser, the limited spatial resolution of the channel-plate detector in the present instrument would prevent the extra resolution from being usefully employed.

For these reasons the experiments on field-ionization were limited to those in which a resolution of 2-4 volts was acceptable, at least in the initial stages.

3.3.1 Field Adsorption: Previous Work.

It was assumed for a long time that the surface of a field-ion emitter was perfectly clean and free from adsorbates, since field-ion micrographs of refractory metals imaged in helium showed perfectly regular crystallographic structures; it was believed that the electric field acted as a barrier by ionizing contaminants, while the helium itself was not expected to be significantly adsorbed at 20°K or 78°K. When 'promoted' images were obtained, in which a helium-ion image of enhanced resolution was obtained at a lower field than normal by adding a few percent of neon or hydrogen to the helium, Muller (1967) attributed the effect to the ability of the promoting gas to act as an intermediate collision partner between the incoming energetic image gas and the cold metal surface, enabling the image gas to be accommodated readily to the specimen temperature.

Following the development of the atom-probe it became apparent that inert gases can be adsorbed for long periods of time on the surface even at relatively high temperatures. Muller, Panitz and McLane (1969) reported that sharp neon and helium peaks were sometimes obtained as well as the metal peaks in the mass spectrum. It was clear that the gases must be adsorbed semipermanently on the surface, in view of the short length of the desorption pulse and the low ambient gas pressure.

Following the introduction of the channel-plate image-intensifier (Turner and co-workers 1969), Schmidt and co-workers (1971) observed 'hopping bright spots' on the field-ion image when neon was added at low pressures ($\sim 10^{-8}$ Torr) to the helium imaging gas. This was attributed to an enhancement of helium ionization when a neon rather than a helium atom was adsorbed on the surface.

Rendulic (1971, 1972) used a photomultiplier to measure screen brightness, and hence quantitatively measured the enhancement produced by adding neon to helium. Rendulic, and Janssen (1973) measured the lifetime of an adsorbed neon atom on the surface under imaging conditions; Janssen showed that the lifetime was given fairly accurately be an equation of the form

$$t = t_o \exp \left(\frac{\frac{1}{2} f_o \alpha F^2 + E_o}{k\,T} \right)$$

where $t_o = 1/\nu_o = 10^{-12} - 10^{-14}$ sec

$E_o = 300\text{-}600$ cal/mole

and f_o is a factor whose derivation will be outlined below. The lifetime at any particular surface site is a large fraction of a second at 78°K, in the presence of helium imaging gas.

Boyes (1971,1974) has observed field-adsorbed films of argon and xenon on iridium, using neon-ion microscopy. He found that the degree of coverage of the specimen surface was a sensitive function of the local field at any point. Some interaction between the xenon atoms was evident, as only complete films were stable; this was not the case for argon films.

Krishnaswamy and Muller (1972,1973) measured the field-ion energy spectrum of helium and neon in the presence of hydrogen. They found that there were ions in the spectrum with higher energies than would normally be observed - that is, ions originating between the metal surface and the normal critical distance for ionization were observed. They attributed these ions to the desorption of field-adsorbed image-gas by the electron shower from hydrogen ionizing far from the specimen surface. This result was not generally acceptable at the time, in view of the small cross-section for electron impact desorption found in other experiments, and the possibility was raised that the high-energy signal was due to a 'ghost' spectral line produced by the Mollenstadt analyser, which is capable of producing such artefacts. It will be confirmed below that the high-energy ions are not produced in this way, but are genuine.

3.3.2 Theory of Field-Adsorption.

The currently-held theory of field-adsorption was put forward by Tsong in 1970. He pointed out that a gas atom which is polarized by the high field at the surface will be attracted to the surface by image forces; providing that the surface atoms are polarizable an electrostatic image dipole will be induced in the surface. This will produce a short-range binding force, in addition to the long-range $\frac{1}{2}\alpha F^2$ binding energy, which confines a thermally-accommodated atom to the vicinity of the high-field region around the specimen. The field experienced by a gas atom of polarizability α_a at a distance d from a metal atom of polarizability α_m is

$$\overline{F}_a = \overline{F}_o + \left(3\hat{n}\,(\overline{p}_m.\hat{n}) - \overline{p}_m\right) / d^3$$

where $\overline{p}_m = \alpha_m \overline{F}_m$, F_o is the applied field, and $\hat{n}$ is a unit vector. Similarly, for the metal atom

$$\overline{F}_m = \overline{F}_o + \left(3\hat{n}\,(\overline{p}_a.\hat{n}) - \overline{p}_a\right) / d^3 \quad .$$

These may be combined to give the potential energy of the gas atom as

$$U_a = -\tfrac{1}{2}\alpha_a F_o^2 \left(\frac{(1 + 2\alpha_m/d^3)^2}{(1 - 4\alpha_m \alpha_a/d^6)} \right)$$

$$\equiv -\tfrac{1}{2}\alpha_a f_a F_o^2$$

Substitution of known values for the atomic radii and polarizabilities, and assuming that $\alpha_m = 3{,}44\ \mathrm{A}^3$, which is derived from experiments on field-evaporation and, as shown in Chapter 1, is subject to some doubt, leads to local adsorption energies, given by $\frac{1}{2}\ \alpha_a(f_a - 1)\ F_o^2$, of 0,13 eV for He at 4,5 v/Å, of 0,14 eV for Ne at 3,75 v/Å, and of 0,15 eV for Ar at 2,2 v/Å. These are of the correct order of magnitude to give lifetimes which are near the experimentally observed values.

While Tsong's theory clearly contains a large part of the truth, it is a simplified version of the real situation. In particular, the use of only the first polarizability α_m may be questioned. Buckingham and Orr (1967) define the energy of a molecule in a field as a power series

$$U \;=\; p\,F \;+\; \tfrac{1}{2}\alpha F^2 \;+\; 1/6\,\beta F^3 \;+\; 1/24\,\gamma F^4 \;+\; .\;.$$

Here p is the permanent dipole moment and β, γ are the first and second hyperpolarizabilities respectively. $\beta = 0$ for all cases in which the molecule has two-fold symmetry, such as, for example, a spherical helium atom. Muller and Tsong (1973) introduce terms in F^4 into a refined version of the simple image force theory of field-evaporation. However, a metal surface atom is not in a symmetric situation; part of it is exposed, and part of it is immersed in the sea of conduction electrons. Under these circumstances it seems unwise to reject terms involving β and F^3 at least until some estimate of the magnitude of β becomes available.

3.3.3 Energy Analysis and Field Adsorption

The position at which the majority of the field-ion current is formed at BIV is given by (Muller and Tsong 1969)

$$e F x_c = I - \phi - e^2 (16\pi\varepsilon_0 x_c)^{-1} + \tfrac{1}{2} F^2 (\alpha_a - \alpha_i)$$

and ions will therefore have an energy deficit

$$\Delta E_{x_c} = \text{potential at point of formation + image potential of the ion}$$

$$= \int_0^{x_c} e\, F(X)\, dx + e^2 (16\pi\varepsilon_0 x_c)^{-1}$$

$$= I - \phi + \text{small polarizability term}$$

An ion formed from an atom which was originally in contact with the metal surface will have a deficit of approximately

$$\Delta E_{ads} \simeq (\lambda + r_{ads})F + e^2(16\pi\varepsilon_0(r_{ads} + \lambda))^{-1}$$

where λ is the penetration depth of the field, of the order of 0,2 to 0,9 A (Taylor 1970), and r_{ads} is the atomic radius of the adsorbate.

The difference in energies of the two ions is then approximately

$$\Delta E = I - \phi - (\lambda + r_{ads}) F - e^2 (16\pi\varepsilon_0(r + \lambda))^{-1}$$

This derivation assumes that none of the kinetic energy of an exciting electron is transferred to the ion desorbed from the surface. This is not necessarily the case. Clampitt (1972) has reported experiments in which inert-gas atoms were adsorbed on a cooled copper substrate, and desorbed by low-energy electrons under zero-field conditions. He found that a proportion of the atoms were desorbed as excited neutrals, with a mean kinetic energy of 4 eV for Ar^* atoms desorbed by 93 eV electrons. The remaining atoms were desorbed as singly-charged ions, with kinetic energies in the range 1-4 eV. The ions are presumed to be formed by resonance ionization (Hagstrum 1964), as the condition $I - I^* \lesssim \phi$ is met; here I is the first ionization potential and

Fig. 3.4.

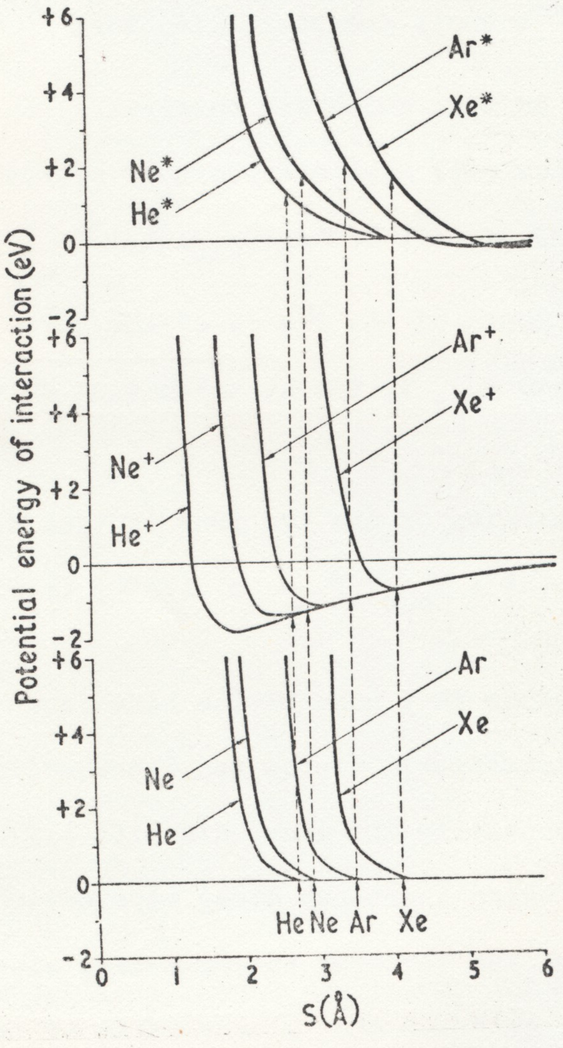

Potential energy of interaction (eV)
+6
+4
+2
0
-2
Ar*
Xe*
Ne*
He*
Ar+
Xe+
Ne+
He+
Ar
Xe
Ne
He
He Ne Ar Xe
0
1
2
3
4
5
6
S(Å)

Fig. 3.5

The field-ion energy spectrum of a helium/hydrogen mixture. The bright area at the top of the photographs is a detector artefact.
a) Helium alone b) Hydrogen alone c) Helium and hydrogen together.

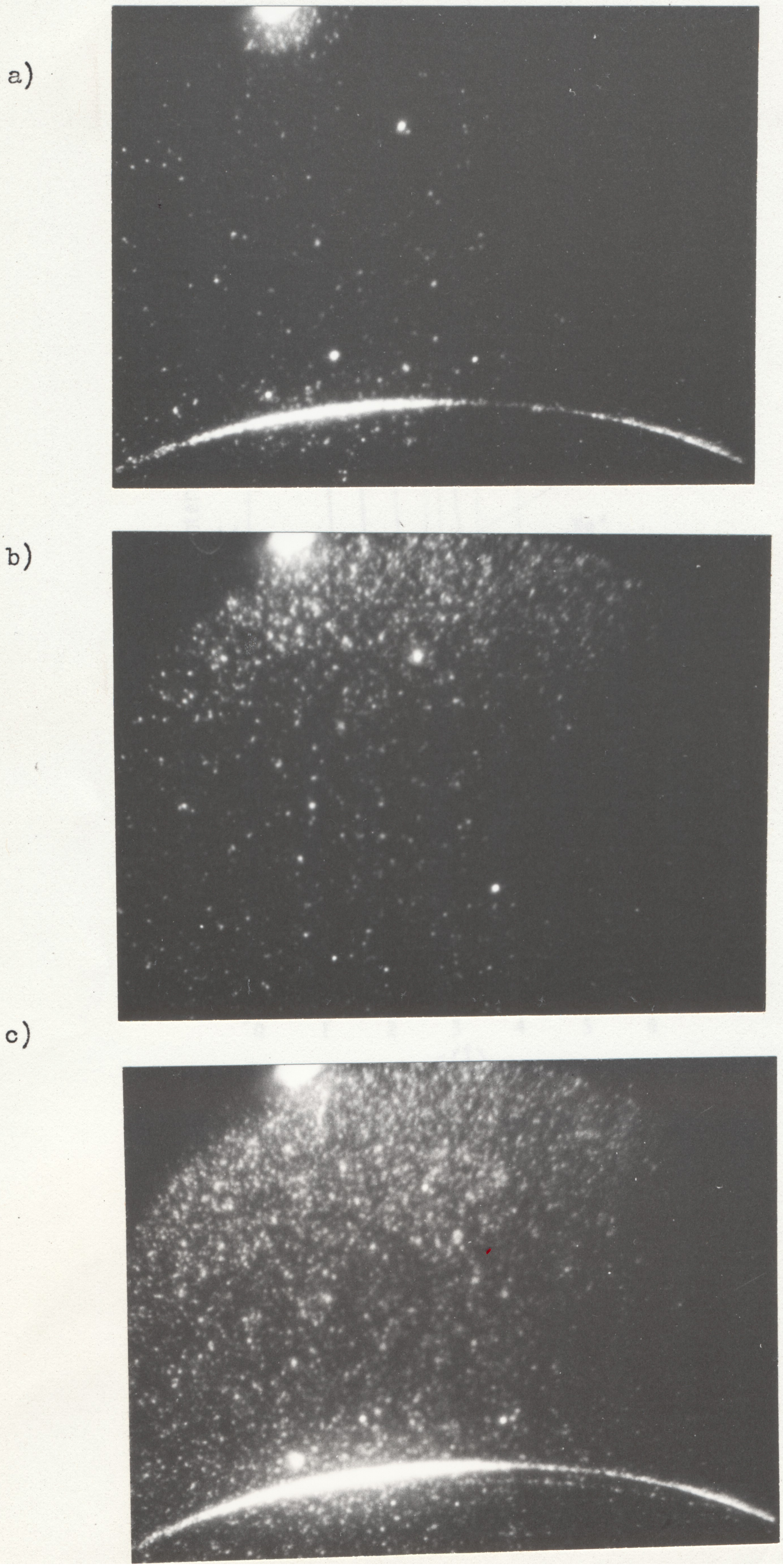

I^* the first excitation energy of the atom, and ϕ is the metal work function. Using these data in conjunction with the potential diagrams of Hagstrum (1954), reproduced in fig(3.4), suggests that the equation for ΔE should be modified ;

$$\Delta E' = I - \phi - (\lambda' + r')\,F - e^2(16\pi\varepsilon_0(r' + \lambda))^{-1} - Q_{KE}$$

where r' is considerably less than the radius of a neutral adsorbate atom and Q_{ke} is a kinetic energy in the range 1-4 eV. The adjustment provided by these new parameters should more than compensate for the fact that the coulomb-attraction image force is not likely to be a very good description of the interaction between the newly-formed ion and the metal surface which is in close proximity. The separation of the spectral lines is expected to be in the range 7 - 15 eV, and to be a decreasing function of the field.

3.3.4 Experimental Results.

The experiment of Krishnaswamy and Muller (1973), in which the energy spectrum of a mixture of hydrogen and helium or neon is observed, was repeated. The results are illustrated by fig (3.5a-c). Fig(3.5a) shows the energy spectrum from helium imaging near to best image field, producing ions of a single energy. If the helium is replaced by hydrogen, at the same field, the spectrum is much broader and at a lower energy, corresponding to ionization far from the surface; the bulk of the hydrogen ion are at too low an energy to be seen in fig(3.5b). If and only if the helium and the hydrogen are present together a second sharp line appears in the spectrum to the high-energy side of the original helium line.

Fig. 3.6

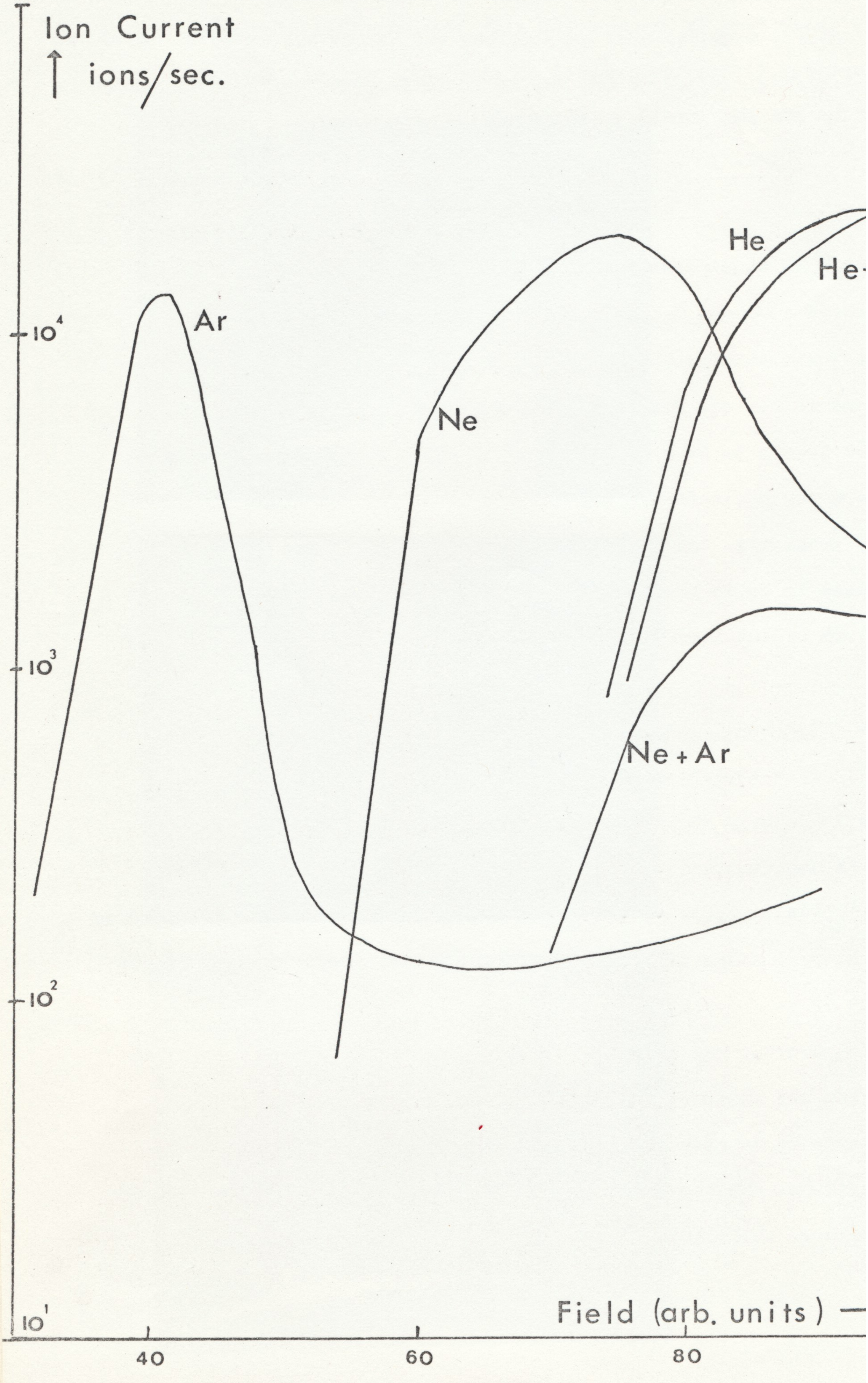
Ion Current
ions/sec.
10^4
10^3
10^2
10^1
Ar
Ne
He
He
Ne + Ar
Field (arb. units)
40
60
80

A similar high-energy line is obtained in a mixture of hydrogen and neon, thereby confirming Krishnaswamy's original experimental results.

It is clear, in view of the high energy and the sharpness of the line, that the ions involved must originate close to the surface. These ions must be either helium or neons ions dislodged by electron impact as outlined, or possibly complex ions (e.g. HeH^+ or NeH^+). An attempt to distinguish between these possibilities, by using field-ionized argon instead of hydrogen as a source of low-energy electrons, was thwarted by the low ion current which could be obtained from the argon at any reasonable pressure, at fields high enough to ionize the helium or neon. Cartwright (1971) has shown that at high fields the majority of the argon is supplied by hopping down the specimen shank (Southon 1963), and a region of intense ionization around the edges of the specimen reduces the argon supply to the specimen endcap. This is ilustrated by a plot of ion current vs. field for various gases and gas mixtures, for a tungsten specimen (fig(3.6)). This was obtained from an auxiliary UHV field-ion microscope equipped with a probe-hole and an electron multiplier/counting system to measure the current (Cartwright measured the total screen current for the inert gases, separately, using a channel-plate/phosphor/external photomultiplier).

The effect of a small quantity of argon on the neon field-ion current is dramatic; observation of the field-ion image under the conditions of fig(3.6) showed that the small number of adsorbed argon atoms image extremely brightly, and apparently drain the local supply of neon atoms away (Boyes 1974): when an adsorbed argon atom was under the probe-hole the current was very much larger (approaching 10^5 ips on the scale of fig(3.6)).

At high fields the argon atom supply to the surface is reduced and the neon-ion current reverts to its normal value.

The main argument which has been advanced against the electron-impact desorption hypothesis is that the cross-section for desorption under zero-field conditions is very low for typical adsorbates, generally being around $5\ 10^{-22}\ m^2$ (Menzel 1975). An estimate of the apparent average desorption cross-section can be made from the energy-spectrum if the intensity of the various peaks is known. An accurate measure of the intensity of a peak can be made by counting the number of scintillations of which it is composed. A hand count of the scintillations in a helium/hydrogen spectrum taken at the lowest field at which appreciable helium ionization occurred (3,3 v/A) revealed 2760 ions in the broad hydrogen peak, 72 in the normal He^+ peak, and 48 in the high-energy peak. Assuming that each electron which is produced by the ionization of hydrogen intersects an adsorbed helium atom at the metal surface (i.e. there is a constant rapid replenishment of the adsorbed film) then the average cross-section (ignoring its variation with electron energy) is 48/2760x(area of a helium atom) $\simeq$ $8,1\ 10^{-22}\ m^2$.

We thus see that the apparent cross-section under these conditions is comparable to that found in electron-impact desorption experiments. Swanson and Crouser(1963) suggested that the low cross-section in zero field is largely due to rapid neutralization of the ion by electron capture from the adjacent metal; it seems possible that the cross-section under field-ion conditions might be slightly greater at higher fields, since the ion is rapidly removed from the vicinity of the metal surface.

Varying the field while the helium/hydrogen spectrum was being observed showed that the normal helium peak and the high-energy peak both faded at the same lower limit, at a field of about 3,3 v/A, which is close to the field at which Muller and coworkers (1969) found that field-adsorbed helium ceased to appear in atom-probe spectra. This is strong confirming evidence that the high-energy signal is due to field-adsorbed helium, and suggests that the presence of the field-adsorbed helium promotes the normal helium-ion current; helium will still be supplied to the surface at lower fields, even if it is not strongly adsorbed. An attempt to measure the separation of the normal and high-energy lines as a function of field, for comparison with the formula derived above, was unsuccessful; the 3-4 volt resolution of the analyser, while allowing it to be seen that the high-energy ions were in the correct energy range, was too poor to allow any meaningful comparison between theory and experiment.

3.3.5 Conclusions and Suggestion for Further Work.

The existence of ions with unexpectedly high energies in the spectra obtained from a mixture of hydrogen and helium or neon is confirmed. The apparent cross-section for desorption, assuming that the electron shower from field-ionized hydrogen is responsible, is found to be at least of the right order of magnitude for the electron-impact theory to be correct. This cannot be proved until it is shown experimentally that the high-energy ions are definitely He^+ or Ne^+, rather than a complex hydride ion. This should be possible to prove using a magnetic spectrometer. An alternative method of proof, the substitution of argon for the hydrogen as a source of low-energy electrons, was found to be made difficult in the present experiments by the low supply of argon ions, and hence electrons, and by the effect on the normal behaviour of the helium and neon due to the bright emission from field-adsorbed argon. Southon (private communication) has suggested that at higher temperatures the argon supply to the specimen endcap at high fields will be increased and also the residence time of adsorbed argon atoms will be decreased. It may be possible in future experiments to strike a balance between the higher argon supply at high temperatures on one hand, and the lower residence time of field-adsorbed helium on the other. Assuming that electron-impact desorption is a rapid process it might also be possible to correlate the arrival of a high-energy ion at a detector with the arrival of a hydrogen ion shortly beforehand, provided that the trajectories of both were suitable.